Nuclear collective motion with a coherent coupling interaction between quadrupole and octupole modes

N. Minkov,[1,*] P. Yotov,[1] S. Drenska,[1] W. Scheid,[2] D. Bonatsos,[3] D. Lenis,[3] and D. Petrellis[3]

[1]*Institute of Nuclear Research and Nuclear Energy, 72 Tzarigrad Road, BG-1784 Sofia, Bulgaria*

[2] *Institut für Theoretische Physik der Justus-Liebig-Universität, Heinrich-Buff-Ring 16, D-35392 Giessen, Germany*

[3] *Institute of Nuclear Physics, N.C.S.R. "Demokritos," GR-15310 Aghia Paraskevi, Attiki, Greece*

A collective Hamiltonian for the rotation-vibration motion of nuclei is considered in which the axial quadrupole and octupole degrees of freedom are coupled through the centrifugal interaction. The potential of the system depends on the two deformation variables β_2 and β_3. The system is considered to oscillate between positive and negative β_3 values by rounding an infinite potential core in the (β_2, β_3) plane with $\beta_2 > 0$. By assuming a coherent contribution of the quadrupole and octupole oscillation modes in the collective motion, the energy spectrum is derived in an explicit analytic form, providing specific parity shift effects. On this basis several possible ways in the evolution of quadrupole-octupole collectivity are outlined. A particular application of the model to the energy levels and electric transition probabilities in alternating parity spectra of the nuclei ^{150}Nd, ^{152}Sm, ^{154}Gd, and ^{156}Dy is presented.

I. INTRODUCTION

Shape deformations and surface oscillations in atomic nuclei determine from a geometric point of view the main features of nuclear collective dynamics [1]. The leading quadrupole mode manifests itself in all regions of collectivity providing vibrational, rotational, and transitional structures of the spectra. In addition, in some regions the manifestation of octupole degrees of freedom is superposed, leading to more complicated shape properties and parity effects in the spectrum of the system [2,3]. A variety of microscopic, geometric, and algebraic model approaches have been applied in nuclear regions where the quadrupole and octupole degrees of freedom coexist [3].

In general, the problem of quadrupole-octupole collectivity is not easy to solve neither microscopically, mainly because of the breaking of reflection symmetry, nor geometrically, because of the difficulty in determining the total inertia tensor of the system. It is, however, simplified considerably if the axial symmetry is still preserved and if the octupole deformations are fixed appropriately with respect to the principal axes of the quadrupole shape. Further simplification is achieved if both degrees of freedom are separated adiabatically. It allows one to examine the manifestation of the octupole mode for fixed values of quadrupole parameters. In such a case the collective motion can be associated to the oscillations of the reflection asymmetric shape with respect to an octupole variable β_3 in a double-well potential [4,5]. Then the parity shift effect observed in nuclear alternating parity bands can be explained as the result of the tunneling through the potential barrier [6,7]. This concept has been generalized for the case of simultaneously contributing quadrupole and octupole modes [8], as well as for the case of higher multipole degrees of freedom [9]. In both cases the double-well potential was

defined in terms of a variable carrying the relative contribution of the different degrees of freedom and not the absolute values of the respective deformation variables. In such a way the explicit form of the original potential in terms of the quadrupole β_2 and octupole β_3 deformation variables was not given. As a consequence, some basic characteristics of the quadrupole and octupole modes and their interaction remain outside of consideration. Such is the behavior of the system in dependence on the quadrupole and octupole stiffness, as well as the limiting case of a frozen quadrupole variable. Another interesting question is if and to what extent one may consider the presence of a tunneling effect in the space of the octupole variable β_3 after the quadrupole coordinate β_2 is let to vary. Some limiting cases in the shape evolution and the angular momentum properties of the system are also of interest in respect with the above.

The purpose of the present work is to clarify the above questions by applying a simple explicit form of the collective energy potential as a function of the quadrupole and octupole axial deformation variables β_2 and β_3. We examine the evolution of the potential shape in dependence on both degrees of freedom, as well as on the collective angular momentum. The geometric analysis suggests that the oscillations of the system in the two-dimensional case of simultaneous manifestation of the quadrupole and octupole modes are performed in a different way, compared to the one-dimensional case of a reflection asymmetric shape with a frozen quadrupole variable. We study the physical consequences of the two-dimensional oscillations and demonstrate their role in the rotation-vibration motion of the system.

In particular, the explicit geometric analysis of the quadrupole-octupole potential suggests a possibility for a coherent interplay between both collective modes. This allows the derivation of explicit analytic expressions for the energy levels and electromagnetic transition probabilities applicable to nuclei in which an "equal" (coherent) manifestation of quadrupole and octupole degrees of freedom is considered.

---

*Electronic address: nminkov@inrne.bas.bg

As a result, one is able to study in detail the respective effects in the structure of the spectrum. Below it will be shown that such a consideration can be applied reasonably to some nuclei in the rare-earth region, such as the $N = 90$ isotones ^{150}Nd, ^{152}Sm, ^{154}Gd, and ^{156}Dy. These nuclei are also a subject of interest [10,11] from the point of view of the X(5) critical point symmetry [12] between quadrupole vibrations [U(5)] and axial quadrupole deformation [SU(3)]. In the present work we shall, however, mainly consider the common quadrupole-octupole collective properties, which, in principle, can take place in various nuclear regions.

In Sec. II the Hamiltonian of the coupled quadrupole and octupole modes is presented, together with the geometric analysis of the quadrupole-octupole potential. In Sec. III the Schrödinger equation is considered in the case of a coherent interplay between the two degrees of freedom. The analytic solutions for several particular forms of the potential and the respective schematic spectra are given in Sec. IV. In addition, results of the model description of alternating parity spectra in ^{150}Nd, ^{152}Sm, ^{154}Gd, and ^{156}Dy are presented. The electric transition probabilities are considered in Sec. V, whereas in Sec. VI a brief discusssion of the influence of the γ degree of freedom on the present results is given. Finally, a summary and concluding remarks are given in Sec. VII.

II. HAMILTONIAN FOR THE COUPLED QUADRUPOLE AND OCTUPOLE MODES

We assume that the system is allowed to oscillate with respect to the quadrupole β_2 and octupole β_3 axial deformation variables. In addition, both degrees of freedom are coupled through a centrifugal (rotation-vibration) interaction depending on the collective angular momentum I. The energy potential represents a two-dimensional surface determined by the variables β_2 and β_3.

The quadrupole-octupole Hamiltonian describing the collective motion under the above assumptions has the form

$$H_{qo} = -\frac{\hbar^2}{2B_2}\frac{\partial^2}{\partial\beta_2^2} - \frac{\hbar^2}{2B_3}\frac{\partial^2}{\partial\beta_3^2} + U(\beta_2, \beta_3, I), \quad (1)$$

where the potential is

$$U(\beta_2, \beta_3, I) = \frac{1}{2}C_2\beta_2^2 + \frac{1}{2}C_3\beta_3^2 + \frac{X(I)}{d_2\beta_2^2 + d_3\beta_3^2}, \quad (2)$$

with $X(I) = I(I+1)/2$. Here B_2 and B_3 are the effective quadrupole and octupole mass parameters and C_2 and C_3 are the stiffness parameters for the respective oscillation modes.

The last term in Eq. (2) provides a coupling between quadrupole and octupole degrees of freedom. Its denominator can be associated to the moment of inertia of an axially symmetric quadrupole-octupole deformed shape, $\mathcal{J}^{(\text{quad+oct})} = 3B_2\beta_2^2 + 6B_3\beta_3^2$ [13]. Therefore, the constants $d_2, d_3 > 0$ can be related to the mass parameters as $d_2 = 3B_2$ and $d_3 = 6B_3$. However, in the present study we do not impose this relation and below a more general correlation between d_2, B_2 and d_3, B_3 is considered. The quantities d_2 and d_3 determine the contributions of the quadrupole and octupole modes, respectively, to the moment of inertia. Also, we remark that

if the ground state of the system is considered ($I = 0$), the potential $U(\beta_2, \beta_3, I)$ should be taken by replacing $X(I) \rightarrow d_0 + X(I)$, with d_0 being a constant.

The Hamiltonian [Eq. (1)] represents a two-dimensional generalization of the soft octupole oscillator Hamiltonian introduced in Ref. [14], as well as of the one-dimensional octupole Hamiltonian derived in Ref. [15]. In the latter two approaches the quadrupole mode is assumed frozen as mentioned in Sec. I. In this respect, Eq. (1) corresponds to an extension in which the quadrupole coordinate is let to vary. Also, it corresponds to the quadrupole-octupole Hamiltonian in Refs. [8,9]. However, in the present work the potential energy [Eq. (2)] is taken in an explicit form depending on β_2 and β_3 (including the harmonic oscillator part), whereas in Refs. [8,9] a double-oscillator potential is defined in the space of polar coordinates. In this way, the explicit form of Eq. (2) allows one to examine in detail the potential surface and its dependence on the model parameters and the collective angular momentum.

Having in mind that the quadrupole deformation has the leading role in the rotation mode, we assume that its contribution to the moment of inertia is larger than the octupole contribution. This assumption corresponds to the condition $d_2 > d_3$, e.g., we can take $d_2 = 0.1\hbar^2\,\text{MeV}^{-1}$ and $d_3 = 0.01\hbar^2\,\text{MeV}^{-1}$. Then, for comparable values of the deformation variables β_2 and β_3, the input of the quadrupole mode in the denominator of the centrifugal term will be larger than the octupole one. However, as shown in Sec. III, this circumstance does not restrict the possibility of equal (coherent) contributions of both degrees of freedom in the mixed quadrupole-octupole oscillation mode. Moreover, because the rotation and vibration modes are coupled, the above condition might be not strictly imposed. In this meaning the considered values of d_2 and d_3 provide only a schematic geometric analysis of the potential [Eq. (2)].

Let us now examine the minimum of the potential energy in dependence on the model parameters. The set of extremum conditions for the coordinates of the two-dimensional minimum ($\beta_{2\min}, \beta_{3\min}$) is

$$\left.\frac{\partial}{\partial\beta_2}U(\beta_2, \beta_3, I)\right|_{(\beta_{2\min}, \beta_{3\min})} = 0 \quad \text{and}$$
$$\left.\frac{\partial}{\partial\beta_3}U(\beta_2, \beta_3, I)\right|_{(\beta_{2\min}, \beta_{3\min})} = 0; \quad (3)$$

$$\left.\frac{\partial^2}{\partial\beta_2^2}U(\beta_2, \beta_3, I)\right|_{(\beta_{2\min}, \beta_{3\min})} > 0 \quad \text{and}$$
$$\left.\frac{\partial^2}{\partial\beta_3^2}U(\beta_2, \beta_3, I)\right|_{(\beta_{2\min}, \beta_{3\min})} > 0. \quad (4)$$

It determines the following possible cases for the bottom of the potential:

(i) $\beta_{3\min} = 0$; $\beta_{2\min} = \pm[2X(I)/(d_2C_2)]^{1/4}$;
(ii) $\beta_{2\min} = 0$; $\beta_{3\min} = \pm[2X(I)/(d_3C_3)]^{1/4}$;
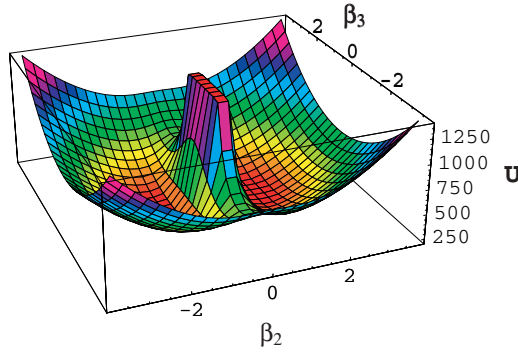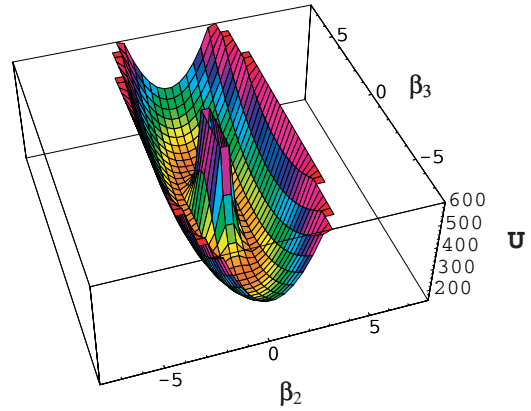
FIG. 1. (Color online) Schematic 3D plot of the potential $U(\beta_2, \beta_3, I)$, Eq. (2), in MeV, for $I = 5$, as a function of β_2 and β_3. The parameter values are $C_2 = C_3 = 100$ MeV, $d_2 = 0.1\hbar^2$ MeV^{-1}, and $d_3 = 0.01\hbar^2$ MeV^{-1}.

(iii) $\beta_{2\min} \neq 0$ and $\beta_{3\min} \neq 0$ with the condition

$$C_2 = \frac{2X(I)d_2}{\left(d_2\beta_{2\min}^2 + d_3\beta_{3\min}^2\right)^2}$$

and

$$C_3 = \frac{2X(I)d_3}{\left(d_2\beta_{2\min}^2 + d_3\beta_{3\min}^2\right)^2}. \tag{5}$$

The shape of the potential corresponding to case (i) is illustrated in Fig. 1. It is characterized by two energy minima for $\beta_2 > 0$ and $\beta_2 < 0$ separated by a well-determined potential barrier. For given sign of β_2 (we consider $\beta_2 > 0$) the bottom of the potential is not separated in the β_3 direction, allowing oscillations of the system between $\beta_3 > 0$ and $\beta_3 < 0$. This situation is illustrated in Fig. 2. We see that for a fixed physically typical value of β_3 [Fig. 2(a)] the barrier in the quadrupole space of β_2 is very large. Thus it restricts the values of the quadrupole deformation within the half space $\beta_2 > 0$. For a fixed typical β_2 value [Fig. 2(b)] the barrier

FIG. 3. (Color online) Schematic 3D plot of the potential $U(\beta_2, \beta_3, I)$, Eq. (2), in MeV, for $I = 5$, as a function of β_2 and β_3. The parameter values are $C_2 = 100$ MeV, $C_3 = 10$ MeV, $d_2 = 0.1\hbar^2$ MeV^{-1}, and $d_3 = 0.01\hbar^2$MeV^{-1}.

in the octupole space of β_3 is relatively small. From Fig. 1 it is seen that for some higher β_2 values this barrier is reduced, and for $\beta_2 \gtrsim \beta_{2\min}$ it disappears ($\beta_{3\min} = 0$).

In case (ii) the potential shape is the same as in Fig. 1, but the coordinates β_2 and β_3 are exchanged. As far as the system is not considered to oscillate between positive and negative β_2 deformations, this case is not of interest in the context of the present analysis.

In the case (iii) of nonzero $\beta_{2\min}$ and $\beta_{3\min}$, Eq. (6) imposes the relation

$$\frac{d_2}{C_2} = \frac{d_3}{C_3}. \tag{6}$$

It determines an elliptic form of the bottom of the two-dimensional potential surface given by $\beta_{2\min}^2/\sqrt{2X(I)/(d_2C_2)} + \beta_{3\min}^2/\sqrt{2X(I)/(d_3C_3)} = 1$. The shape of the potential corresponding to case (iii) is illustrated in Fig. 3. It suggests that the system moves in the two-dimensional space of the deformation variables β_2 and β_3 by rounding the
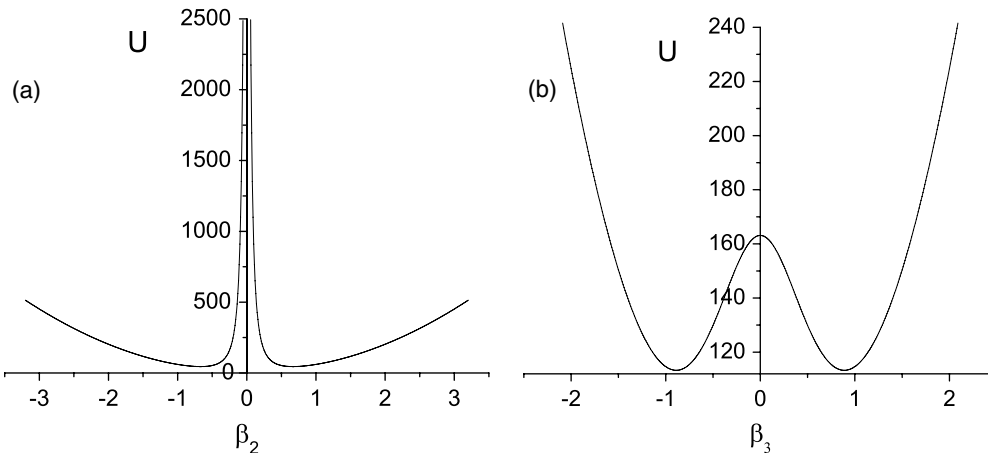

FIG. 2. Schematic numerical behavior of the potential $U(\beta_2, \beta_3, I)$, Eq. (2), in MeV, for $I = 1$, as a function of (a) β_2 at fixed $\beta_3 = 0.1$ and (b) β_3 at fixed $\beta_2 = 0.25$. The parameter values are $C_2 = C_3 = 100$ MeV, $d_2 = 0.1\hbar^2$ MeV^{-1}, and $d_3 = 0.01\hbar^2$ MeV^{-1}.
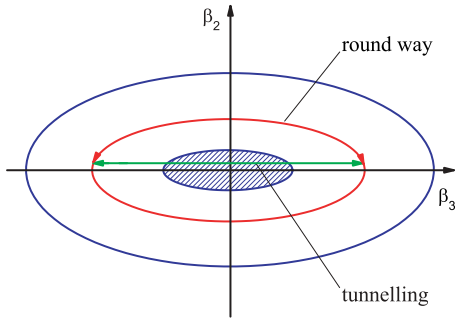
FIG. 4. (Color online) Schematic picture of the tunneling and the rounding way in the β_3 variable. See Sec. II for further discussion.

FIG. 5. (Color online) 3D plot of the potential $U_I(\beta_2, \beta_3)$, Eq. (8), in MeV, for $I = 5$, as a function of β_2 and β_3, with $\beta_{2\,\mathrm{min}} = 0.25$, $\beta_{3\,\mathrm{min}} = 0.1$, $d_2 = 0.1\hbar^2\,\mathrm{MeV}^{-1}$, and $d_3 = 0.01\hbar^2\,\mathrm{MeV}^{-1}$.

internal potential core. If a *prolate quadrupole deformation* is considered, the rounding is performed between positive and negative β_3 values in the space of $\beta_2 > 0$. This situation can be considered as the two-dimensional extension of the one-dimensional case in which the β_2 coordinate is frozen. To explain this in detail, we consider a horizontal (equipotential) intersection of the shape in Fig. 3, which is illustrated schematically in Fig. 4. We see that if the quadrupole coordinate is fixed at some value of $\beta_2 > 0$, the motion in the octupole coordinate between positive and negative β_3 values is characterized by the tunneling through a potential barrier (a vertical intersection of the core). When β_2 is let to vary, the tunneling is replaced by a motion along the curved way rounding the potential core.

The above case (iii) is of particular interest, because of the simultaneous presence of nonzero coordinates of the potential minimum in both degrees of freedom. It suggests that the oscillations in the quadrupole and octupole coordinates are involved in the collective motion on the same footing. As it will be seen below, such a situation appears to take place in certain nuclear regions. Moreover, it will be seen that the ellipsoidal symmetry in the potential bottom allows, under some additional conditions, a *complete analytic determination* of the energy spectrum. This is why in the following we imply this case, unless something different is indicated. Also, we assume only the presence of prolate quadrupole deformations. This is why hereafter we consider only the $\beta_2 > 0$ part of the space.

Further, we examine the evolution of the potential shape with the angular momentum I. We consider the following two cases:

(a) The potential minimum (the two-dimensional bottom) is allowed to change with I for fixed values of the stiffness parameters C_2 and C_3.

(b) The minimum is fixed, so that the values $\beta_{2\,\mathrm{min}}$ and $\beta_{3\,\mathrm{min}}$ determine an ellipse which does not change with the angular momentum.

It is clear that in the case of fixed stiffness parameters, case (a) the quadrupole and the octupole deformations corresponding to the potential minimum should exhibit an overall increase in the denominator of Eqs. (6) with increasing I.

In the case of fixed minima, case (b) the stiffness parameters $C_2 \equiv C_2(I)$ and $C_3 \equiv C_3(I)$ increase quadratically with I
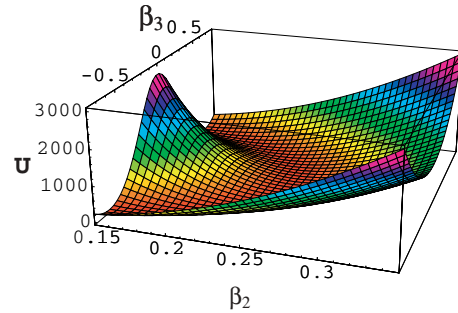
according to the right-hand sides of (6). Then the substitution of Eqs. (6) into (2), leads to the following form of the quadrupole-octupole potential

$$U(\beta_2,\beta_3,I) = X(I)\left[\frac{d_2\beta_2^2 + d_3\beta_3^2}{\left(d_2\beta_{2\,\mathrm{min}}^2 + d_3\beta_{3\,\mathrm{min}}^2\right)^2} + \frac{1}{d_2\beta_2^2 + d_3\beta_3^2}\right].$$
(7)

If the origin of the energy scale is fixed at the potential minimum, one has

$$
\begin{aligned}
U_I(\beta_2,\beta_3) &= U(\beta_2,\beta_3,I) - U(\beta_{2\,\mathrm{min}},\beta_{3\,\mathrm{min}},I) \\
&= \frac{X(I)\left[d_2\left(\beta_2^2 - \beta_{2\,\mathrm{min}}^2\right) + d_3\left(\beta_3^2 - \beta_{3\,\mathrm{min}}^2\right)\right]^2}{\left(d_2\beta_{2\,\mathrm{min}}^2 + d_3\beta_{3\,\mathrm{min}}^2\right)^2\left(d_2\beta_2^2 + d_3\beta_3^2\right)}.
\end{aligned}
$$
(8)

We remark that Eq. (7) includes the rotational contribution of the centrifugal term, which moves up the energy with increasing angular momentum I. However, in Eq. (8) the explicit contribution of the rotational degree of freedom is diminished, so that the energy term keeps mainly the vibrational component. The shape of Eq. (8) with $\beta_2 > 0$ is illustrated in Fig. 5.

III. MODEL POTENTIALS AND THE SCHRÖDINGER EQUATION IN POLAR VARIABLES

Further, it is convenient to introduce polar variables η and ϕ by taking

$$\beta_2 = \frac{\eta}{\sqrt{d_2/d}}\cos\phi; \qquad \beta_3 = \frac{\eta}{\sqrt{d_3/d}}\sin\phi,$$
(9)

with $d = (d_2 + d_3)/2$. Considering $\beta_2 > 0$, we have

$$\eta = \frac{1}{\sqrt{d}}\sqrt{d_2\beta_2^2 + d_3\beta_3^2}; \qquad \phi = \arctan\left(\frac{\beta_3}{\beta_2}\sqrt{\frac{d_3}{d_2}}\right),$$
(10)

where the "effective" deformation variable η is defined with positive values $\eta > 0$, whereas the relative ("angular") variable ϕ is defined in the interval $-\pi/2 \leqslant \phi \leqslant \pi/2$. We remark that the negative ϕ values correspond to negative β_3. (The variable β_3 takes both positive and negative values.)

Then the quadrupole-octupole Hamiltonian (1) can be written in the form

$$
\begin{aligned}
H_{qo} = {} & -\frac{\hbar^2 d_2}{2d B_2}\left[\cos^2\phi\frac{\partial^2}{\partial\eta^2} + \frac{1}{\eta}\sin^2\phi\frac{\partial}{\partial\eta} + \frac{1}{\eta^2}\sin^2\phi\frac{\partial^2}{\partial\phi^2}\right.\\
& + 2\frac{1}{\eta^2}\sin\phi\cos\phi\frac{\partial}{\partial\phi} - 2\frac{1}{\eta}\sin\phi\cos\phi\frac{\partial^2}{\partial\eta\partial\phi}\Big]\\
& - \frac{\hbar^2 d_3}{2d B_3}\left[\sin^2\phi\frac{\partial^2}{\partial\eta^2} + \frac{1}{\eta}\cos^2\phi\frac{\partial}{\partial\eta}\right.\\
& + \frac{1}{\eta^2}\cos^2\phi\frac{\partial^2}{\partial\phi^2} - 2\frac{1}{\eta^2}\sin\phi\cos\phi\frac{\partial}{\partial\phi}\\
& + 2\frac{1}{\eta}\sin\phi\cos\phi\frac{\partial^2}{\partial\eta\partial\phi}\Big] + U_I(\eta).
\end{aligned}
\tag{11}
$$

Under Eq. (6), the potential energy depends only on the effective deformation variable η and on the angular momentum I and not on the relative (angular) variable ϕ. Then in case (a) of fixed stiffness parameters one has

$$
U_I(\eta) = \frac{1}{2}C\eta^2 + \frac{X(I)}{d\eta^2}\qquad\text{[case(a)]},
\tag{12}
$$

where C is defined according to Eq. (6) as $1/C = d_2/(dC_2) = d_3/(dC_3)$.

In case (b) of fixed minima the potential term appears in the following two forms

$$
U_I(\eta) = X(I)\frac{\eta^4 + \eta_{\min}^4}{d\eta_{\min}^4\eta^2}\qquad\text{[case(b1)]}
\tag{13}
$$

$$
U_I(\eta) = X(I)\frac{\left[\eta^2 - \eta_{\min}^2\right]^2}{d\eta_{\min}^4\eta^2}\qquad\text{[case(b2)]},
\tag{14}
$$

where Eq. (13) corresponds to the rotation-dependent potential (7), whereas Eq. (14) represents the essentially vibrational term (8). The quantity $\eta_{\min} = (1/\sqrt{d})(d_2\beta_{2\min}^2 + d_3\beta_{3\min}^2)^{1/2}$ is the value of the variable η in the potential minimum. In the following we refer to Eq. (13) as case (b1) and to Eq. (14) as case (b2).

Using the effective deformation variable η we also examine a third case (c) of an infinite square well with an infinite core at zero defined as

$$
U_w^I(\eta) = \begin{cases}\dfrac{X(I)}{d\eta^2} & \eta \leqslant \eta_w\\[2mm]\infty & \eta > \eta_w\end{cases}\qquad\text{[case(c)]},
\tag{15}
$$

where η_w is a parameter determining the width of the well.

Now we assume the following relation between the quadrupole and octupole mass and inertia parameters

$$
\frac{d_2}{dB_2} = \frac{d_3}{dB_3} = \frac{1}{B}.
\tag{16}
$$

This leads to the following form of the model Hamiltonian

$$
H_{qo} = -\frac{\hbar^2}{2B}\left[\frac{\partial^2}{\partial\eta^2} + \frac{1}{\eta}\frac{\partial}{\partial\eta} + \frac{1}{\eta^2}\frac{\partial^2}{\partial\phi^2}\right] + U_I(\eta).
\tag{17}
$$

The assumption (16), which much simplifies the problem, suggests that d_2 and d_3 are related to the mass parameters B_2 and B_3, respectively, through the same coefficient d/B. By comparing Eq. (16) and Eq. (6), we obtain $C_2/B_2 = C_3/B_3$ or $\omega_2^2 = \omega_3^2$, i.e., Eq. (16) implies that both degrees of freedom,

quadrupole and octupole, are characterized by equal angular frequencies ω_2 and ω_3, respectively. This means that a *coherent interplay* between the two collective modes is assumed. In other words, the Eq. (16) suggests that the oscillations in the quadrupole and octupole coordinates are represented in the collective motion on the same footing. The quantity B in Eq. (16) has the meaning of the effective mass of the total quadrupole-octupole system.

The Schrödinger equation for the Hamiltonian (17) has the form

$$
\begin{aligned}
& -\frac{\hbar^2}{2B}\frac{1}{\eta^2}\left[\eta^2\frac{\partial^2}{\partial\eta^2} + \eta\frac{\partial}{\partial\eta} + \frac{\partial^2}{\partial\phi^2}\right]\Phi(\eta,\phi)\\
& \qquad + U_I(\eta)\Phi(\eta,\phi) = E\Phi(\eta,\phi).
\end{aligned}
\tag{18}
$$

After dividing it by $\hbar^2/(2B\eta^2)$ and separating the variables η and ϕ through $\Phi(\eta,\phi) = \psi(\eta)\varphi(\phi)$ we obtain the following two equations

$$
\frac{\partial^2}{\partial\eta^2}\psi(\eta) + \frac{1}{\eta}\frac{\partial}{\partial\eta}\psi(\eta) + \frac{2B}{\hbar^2}\left[E - \frac{\hbar^2}{2B}\frac{k^2}{\eta^2} - U_I(\eta)\right]\psi(\eta) = 0;
\tag{19}
$$

$$
\frac{\partial^2}{\partial\phi^2}\varphi(\phi) + k^2\varphi(\phi) = 0,
\tag{20}
$$

where k is the separation quantum number.

IV. ANALYTIC SOLUTIONS AND NUMERICAL RESULTS

In the following we give analytic solutions of the above equations in the cases (a)–(c) with the potentials described by Eqs. (12), (13), (14), and (15).

In Case (a), after introducing the potential described in Eq. (12) into Eq. (19) we have

$$
\begin{aligned}
& \frac{\partial^2}{\partial\eta^2}\psi(\eta) + \frac{1}{\eta}\frac{\partial}{\partial\eta}\psi(\eta) + \frac{2B}{\hbar^2}\left[E - \frac{\hbar^2}{2B}\frac{k^2}{\eta^2}\right.\\
& \qquad \left. - \frac{1}{2}C\eta^2 - \frac{X(I)}{d\eta^2}\right]\psi(\eta) = 0.
\end{aligned}
\tag{21}
$$

By introducing a reduced energy $\varepsilon = 2B/\hbar^2 E$ and a reduced angular momentum factor $\widetilde{X}(I) = bX(I)$, with $b = 2B/\hbar^2 d$, we obtain Eq. (21) in the form

$$
\begin{aligned}
& \frac{\partial^2}{\partial\eta^2}\psi(\eta) + \frac{1}{\eta}\frac{\partial}{\partial\eta}\psi(\eta) + \left[\varepsilon - \frac{k^2 + \widetilde{X}(I)}{\eta^2} - \frac{BC}{\hbar^2}\eta^2\right]\\
& \qquad \times \psi(\eta) = 0.
\end{aligned}
\tag{22}
$$

The effective potential appearing in the brackets of Eq. (22) is of a form similar to the Davidson potential [16], which is analytically solvable [17,18]. Thus Eq. (22) can be solved analytically and we obtain the following explicit expression for the energy spectrum

$$
E_{n,k}(I) = \hbar\omega\left[2n + 1 + \sqrt{k^2 + \widetilde{X}(I)}\right],
\tag{23}
$$

where $\omega = \sqrt{C/B}$ and $n = 0, 1, 2, \ldots$. The eigenfunctions $\psi(\eta)$ of Eq. (21) are obtained in terms of the Laguerre

polynomials

$$\psi_n^I(\eta) = \sqrt{\frac{2\Gamma(n+1)}{\Gamma(n+2s+1)}} e^{-a\eta^2/2} a^s \eta^{2s} L_n^{2s}(a\eta^2), \qquad (24)$$

where $a = \sqrt{BC}/\hbar$ and $s = \sqrt{k^2 + \widetilde{X}(I)}/2$.

Now we remark that Eq. (20) in the variable ϕ is solved under the periodic boundary condition $\varphi(\phi + 2\pi) = \varphi(\phi)$. However, the assumption $\beta_2 > 0$, which is equivalent to the consideration of an infinite potential wall at $\beta_2 = 0$ (or $\phi = \pm\pi/2$), imposes the additional condition

$$\varphi(-\pi/2) = \varphi(\pi/2) = 0. \qquad (25)$$

Equation (20) has two different solutions satisfying Eq. (25) with positive, $\pi = (+)$, and negative, $\pi = (-)$, parity as follows

$$\varphi^+(\phi) = \sqrt{2/\pi}\cos(k\phi), \quad k = \pm 1, \pm 3, \pm 5, \ldots; \quad (26)$$

$$\varphi^-(\phi) = \sqrt{2/\pi}\sin(k\phi), \quad k = \pm 2, \pm 4, \pm 6, \ldots. \quad (27)$$

Equation (26) provides positive parity for the intrinsic wave function, whereas Eq. (27) corresponds to a negative parity function. As a result, the intrinsic wave function appears in the form $\Phi^\pm(\eta, \phi) = \psi(\eta)\varphi^\pm(\phi)$. However, the $\mathcal{RP}$ symmetry of the total wave function of the system, $\Psi \sim \Phi^\pm(\eta, \phi)|IKM\rangle$, has to be conserved. The $\mathcal{R}$ symmetry of the rotation function $|IKM\rangle$ is characterized by the factor $(-1)^I$. For the total state of the system one has $\pi(-1)^I = 1$. It follows that for $I =$ even the quantum number k is allowed to take the values $k_{(+)} = 1, 3, 5, \ldots$, corresponding to the even function (26), whereas for $I =$ odd one has $k_{(-)} = 2, 4, 6, \ldots$ corresponding to the odd function (27). Thus, when the angular momentum is changed from $I =$ odd to $I =$ even and vice versa, the respective values of the quantum number k should switch between $k_{(-)}$ and $k_{(+)}$. This parity effect provides an odd-even staggering structure of the spectrum (23). We consider that the lowest states of the system with respect to the variable ϕ are characterized by the lowest k values, $k_{(+)} = 1$ for $I =$ even and $k_{(-)} = 2$ for $I =$ odd. Therefore, the staggering behavior of the model spectrum is provided by the difference $\Delta k^2 = k_{(-)}^2 - k_{(+)}^2 = 3$.

In such a way the energy expression (23), with the parity-dependent quantum number k, determines the structure of an alternating parity spectrum. The energy levels $E_{0,k}(I)$, with $n = 0$, correspond to the yrast alternating parity sequence. The levels with $n \neq 0$ correspond to higher-energy bands, in which the rotational states are built on quadrupole-octupole (mixed β_2-β_3) vibrations of the system. In this case, the states with even I appear similarly to the states of a higher β (quadrupole) band. Thus, the present model suggests that, in the nuclear regions with quadrupole-octupole collectivity, one may consider "octupole mixed" β-band structures. We remark that, in the present model framework, the γ bands are not included. This can be done in an extended formalism allowing the simultaneous consideration of the γ variable. In addition, the octupole triaxiality can be taken into account. Then one may also discuss possible "octupole admixtures" in the γ-band structure.

We can estimate analytically the staggering effect at higher angular momenta, where $\Delta k^2 \ll \widetilde{X}(I)$. The square-
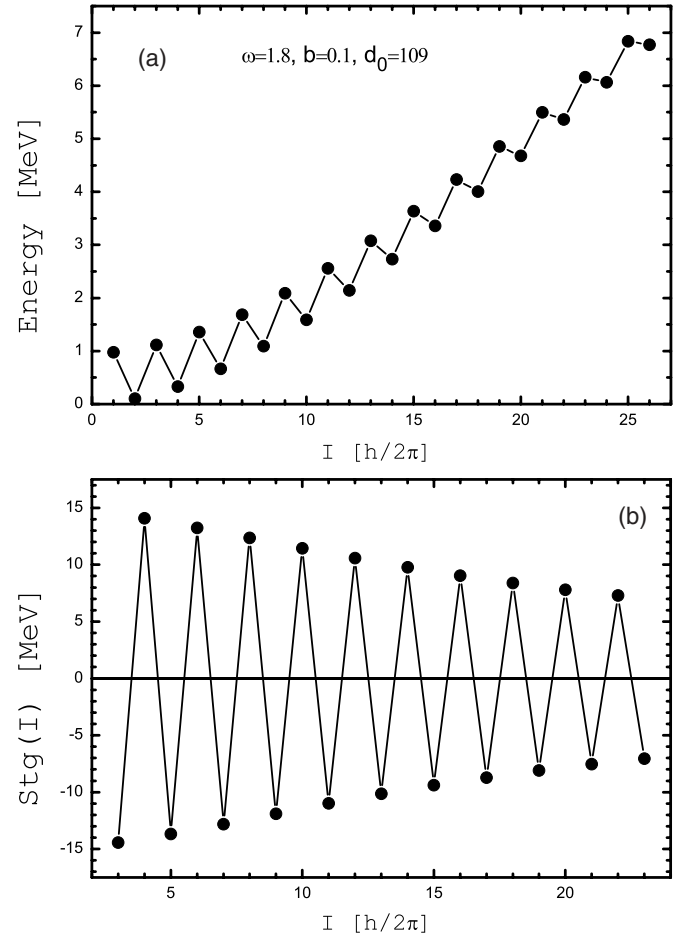

FIG. 6. Schematic energy levels (a) and staggering pattern (b) for the spectrum of Eq. (23) with $n = 0$. The parameter values are shown in (a), ω is given in MeV$/\hbar$, whereas b and d_0 are in $\hbar^{-2}$ and $\hbar^2$ respectively.

root term $\sqrt{k^2 + \widetilde{X}(I)}$ in Eq. (23) can be expanded as $\sqrt{\widetilde{X}(I)} + k^2/[2\sqrt{\widetilde{X}(I)}]$. We see that the term $k^2/[2\sqrt{\widetilde{X}(I)}]$, which is responsible for the staggering effect, decreases nearly linearly with the angular momentum I because $\widetilde{X}(I) = bX(I) \sim I(I+1)$. We consider the quantity $b = 2B/(\hbar^2 d)$ as a model parameter. The numerical behavior of the energy and the staggering effect for the spectrum (23) is illustrated in Fig. 6. The staggering effect is illustrated in terms of the five-point quantity

$$\begin{aligned} \mathrm{Stg}(I) = {} & 6\Delta E(I) - 4\Delta E(I-1) - 4\Delta E(I+1) \\ & + \Delta E(I+2) + \Delta E(I-2), \end{aligned} \qquad (28)$$

where $\Delta E(I) = E(I+1) - E(I)$. The schematic staggering pattern suggests that the odd and even angular momentum sequences approach each other toward higher angular momenta. It outlines a trend for the forming of an octupole band. However, the linear decrement of the staggering amplitude is not enough to provide such a band structure at reasonable (experimentally observed) angular momenta. A similar situation is observed in rare-earth nuclei, where the alternating parity levels approach each other without merging into a single band.
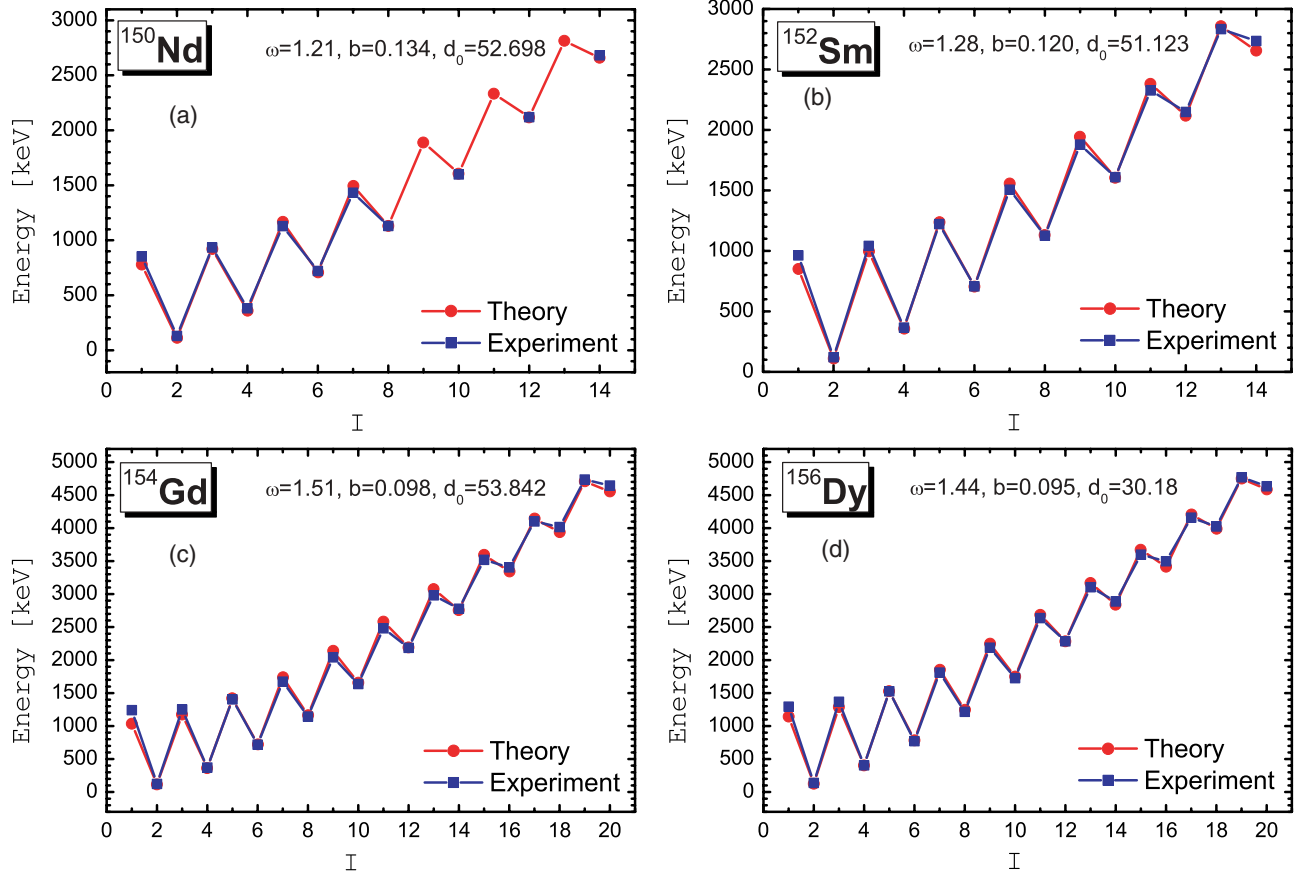
FIG. 7. (Color online) Theoretical and experimental energy levels for the alternating parity bands in ^{150}Nd (data from Ref. [19]), ^{152}Sm (data from Ref. [20], ^{154}Gd (data from Ref. [21]), and ^{156}Dy (data from [22]). The theoretical results are obtained by (23) with $n = 0$. The parameter units are as in Fig. 6.

On this basis, we applied Eq. (23) to describe the alternating parity spectra in the nuclei ^{150}Nd, ^{152}Sm, ^{154}Gd, and ^{156}Dy. The theoretical energies are obtained by taking $\widetilde{E}_{n,k}(I) = E_{n,k}(I) - E_{n,k}(0)$, with $n = 0$ and $X(I) = \frac{1}{2}[d_0 + I(I + 1)]$, where the parameter d_0 characterizes the potential shape in the ground state, as mentioned in the paragraph after Eq. (2). The parameters ω, b, and d_0 are adjusted to the energy levels by means of a least-squares minimization procedure.

In Fig. 7 results for the energy levels of ^{150}Nd, ^{152}Sm, ^{154}Gd, and ^{156}Dy are compared to the experimental data. The respective theoretical and experimental staggering patterns are compared in Fig. 8. In ^{150}Nd [Fig. 7(a)], the levels with $I = 9, 11, 13$ are predicted. The respective staggering pattern for $I > 5$ [Fig. 8(a)] is also predicted. We see that in the nuclei ^{152}Sm, ^{154}Gd, and ^{156}Dy the experimental patterns confirm the predicted behavior of alternating parity levels with increasing angular momentum.

In case (b1) after introducing Eq. (13) into Eq. (19), we have the equation

$$\frac{\partial^2}{\partial\eta^2}\psi(\eta) + \frac{1}{\eta}\frac{\partial}{\partial\eta}\psi(\eta) + \frac{2B}{\hbar^2}\left[E - \frac{\hbar^2}{2B}\frac{k^2}{\eta^2}\right.$$
$$\left. - \frac{X(I)}{d\eta^2} - \frac{X(I)}{d\eta_{\min}^4}\eta^2\right]\psi(\eta) = 0, \qquad (29)$$

which is solved in the same way as Eq. (21) of case (a), and the respective energy levels are obtained in the form

$$E_{n,k}(I) = \hbar^2\frac{\sqrt{\widetilde{X}(I)}}{B\eta_{\min}^2}\left[2n + 1 + \sqrt{k^2 + \widetilde{X}(I)}\right], \qquad (30)$$

where $n = 0, 1, 2, \ldots$. The eigenfunctions $\psi(\eta)$ of Eq. (29) are of the same form as Eq. (24) in case (a), but with $a = \sqrt{\widetilde{X}(I)}/\eta_{\min}^2$.

All considerations related to the ϕ equation (20) and the quantum number k are the same as in case (a). However, now we obtain a different behavior of the staggering amplitude as a function of the angular momentum. This is seen after expanding the term $\sqrt{\widetilde{X}(I)}\sqrt{k^2 + \widetilde{X}(I)}$ of Eq. (30) in the form $\widetilde{X}(I) + k^2/2$. The appearance of the staggering effect is only because of the term $k^2/2$. Because the difference $\Delta k^2 = 3$ does not depend on I, the staggering effect will be characterized by a *constant* amplitude. The schematic behavior of the energy levels and the respective staggering pattern for the spectrum of Eq. (30) are illustrated in Fig. 9. Indeed, we see from Fig. 9(b) that, after some slight increase in the beginning, toward the higher angular momenta the staggering amplitude saturates to a constant value.
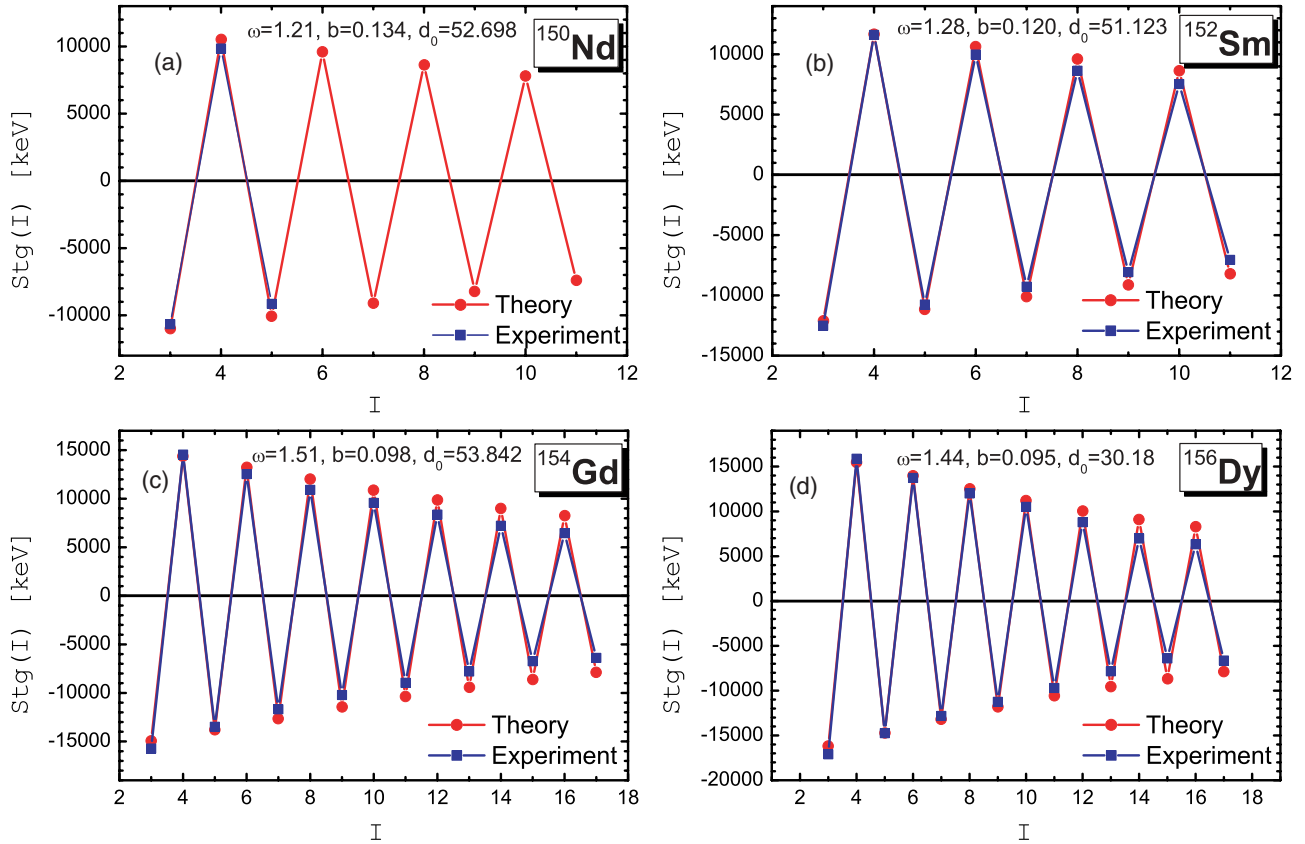
FIG. 8. (Color online) Theoretical and experimental staggering patterns for the alternating parity bands in ^{150}Nd, ^{152}Sm, ^{154}Gd, and ^{156}Dy. Experimental data are taken from the same references as in Fig. 7. The theoretical results are obtained by (23) with $n = 0$. The parameter units are as in Fig. 6.

In case (b2), Eq. (14) differs from Eq. (13) of case (b1) by the term $-2X(I)/(d\eta_{\min}^2)$. The respective energy spectrum is

$$E_{n,k}(I) = \hbar^2 \frac{\sqrt{\widetilde{X}(I)}}{B\eta_{\min}^2}\left[2n + 1 + \sqrt{k^2 + \widetilde{X}(I)} - \sqrt{\widetilde{X}(I)}\right], \quad (31)$$

with the wave function $\psi(\eta)$ being the same as in case (b1). Equation (31) differs from Eq. (30) by the term $-\sqrt{\widetilde{X}(I)}$ in the brackets. This term reduces the angular momentum dependence of the energy to a linear (vibrational) behavior. However, it does not affect the staggering effect. Therefore, similarly to case (b1), the staggering pattern for the levels [Eq. (31)] will be characterized by a constant amplitude. This is seen from the schematic numerical results illustrated in Fig. 10.

In Case (c) (the square-well potential [Eq. (15)] the Schrödinger equation can be written in the form

$$\frac{\partial^2}{\partial\eta^2}\psi(\eta) + \frac{1}{\eta}\frac{\partial}{\partial\eta}\psi(\eta) + \left[\varepsilon - \frac{v^2}{\eta^2}\right]\psi(\eta) = 0, \quad (32)$$

where $v^2 = k^2 + \widetilde{X}(I)$ and $\eta \leqslant \eta_w$. By introducing new variables through the definitions $z = \eta\kappa$ and $\varepsilon = \kappa^2$, we obtain Eq. (32) in the form of the Bessel equation

$$\frac{\partial^2}{\partial z^2}\psi(z) + \frac{1}{z}\frac{\partial}{\partial z}\psi(z) + \left(1 - \frac{v^2}{z^2}\right)\psi(z) = 0. \quad (33)$$

The spectrum of this equation is determined by the boundary condition $\psi_v(\eta_w) = 0$ and is given by

$$\varepsilon = \kappa_{v,n}^2, \qquad \kappa_{v,n} = \frac{x_{v,n}}{\eta_w}, \quad (34)$$

where $x_{v,n}$ is the nth zero of the Bessel function $J_v(z)$. The eigenfunctions have the form $\psi_{v,n}(\eta) = c_{v,n}J_v(\kappa_{v,n}\eta)$, where $c_{v,n}$ are normalization constants. The schematic behavior of the spectrum [Eq. (34)] and the respective staggering pattern are illustrated in Fig. 11. We remark that the staggering amplitude initially decreases, whereas toward higher I it saturates to a constant value.

V. ELECTRIC TRANSITION PROBABILITIES

The formalism developed so far allows the calculation of $E1$, $E2$, and $E3$ transition probabilities for the energy spectra in the considered cases (a)–(c). In cases (a) and (b), the reduced probability for an electric transition of multipolarity L from a state with angular momentum I_i to a state with I_f is given by

$$B(EL; I_i \to I_f) = \frac{1}{2I_i + 1}\sum_{M_i M_f \mu}\left|\left\langle\Phi_{n_f I_f M_f}^{\pm}(\eta, \phi)\right|\right.$$
$$\times \mathcal{M}_\mu(EL)\left|\Phi_{n_i I_i M_i}^{\pm}(\eta, \phi)\right\rangle\right|^2, \quad (35)$$
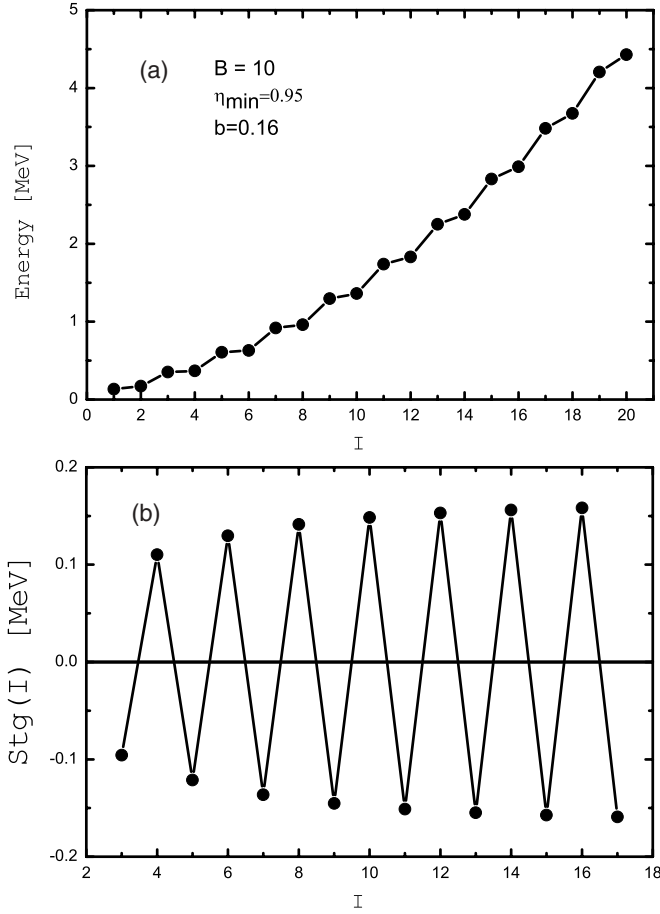
FIG. 9. Schematic energy levels (a) and staggering pattern (b) for the spectrum of Eq. (30) with $n = 0$. The parameter values are shown in part (a), B is given in $\hbar^2/$MeV, b in $\hbar^{-2}$, whereas $\eta_{\min}$ is dimensionless.

where

$$
\Phi^{\pm}_{nIM}(\eta, \phi) = \psi^I_n(\eta)\varphi^{\pm}(\phi)|I0M\rangle
$$

$$
= \sqrt{\frac{2\Gamma(n+1)}{\Gamma(n+2s+1)}}e^{(-a\eta^2/2)}a^s\eta^{2s}L_n^{2s}(a\eta^2)
$$

$$
\times \varphi^{\pm}(\phi)\sqrt{\frac{2I+1}{32\pi^2}}D^I_{0,M}(\theta). \tag{36}
$$

The general form of the multipole operators $\mathcal{M}$ in the collective variables is given in Ref. [23]. The electric quadrupole and octupole transition operators for an axially symmetric nucleus are defined by the deformation variables β_2 and β_3 as

$$
\mathcal{M}_\mu(EL) = M_L\beta_L D^L_{0\mu}(\theta), \qquad L = 2, 3,
$$
$$
(\mu = -L, \ldots, L), \tag{37}
$$

whereas the $E1$ (dipole) transition operator is defined as [24–27]

$$
\mathcal{M}_\mu(E1) = M_1\beta_2\beta_3 D^1_{0\mu}(\theta), \qquad (\mu = 0, \pm 1), \tag{38}
$$

where M_i $(i = 1, 2, 3)$ are constants related to the respective intrinsic moments. In terms of the polar variables η and ϕ the
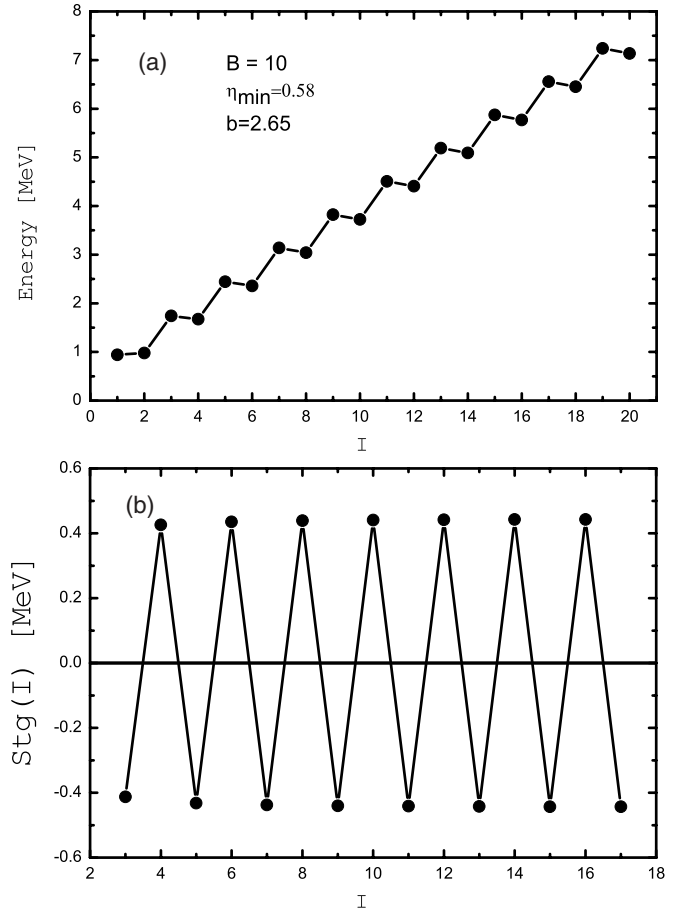
FIG. 10. Same as Fig. 9, but for the spectrum of Eq. (31).

above transition operators read

$$
\mathcal{M}_\mu(E1) = M_1\frac{\eta^2\cos\phi\sin\phi}{\sqrt{d_2d_3/d^2}}D^1_{0\mu}(\theta), \tag{39}
$$

$$
\mathcal{M}_\mu(E2) = M_2\frac{\eta\cos\phi}{\sqrt{d_2/d}}D^2_{0\mu}(\theta), \tag{40}
$$

$$
\mathcal{M}_\mu(E3) = M_3\frac{\eta\sin\phi}{\sqrt{d_3/d}}D^3_{0\mu}(\theta). \tag{41}
$$

In Eq. (35) the integration over the angles θ involves an integral over three Wigner functions [28], which leads to the Clebsch-Gordan coefficients $\langle I_i 0L0|I_f 0\rangle$. The integration over the variable ϕ leads to the following constants

$$
I^{++}_{E2} = \frac{2}{\pi}\int_{-\pi/2}^{\pi/2}\cos^3\phi\,d\phi = \frac{8}{3\pi}, \tag{42}
$$

$$
I^{--}_{E2} = \frac{2}{\pi}\int_{-\pi/2}^{\pi/2}\cos\phi\sin^2(2\phi)\,d\phi = \frac{32}{15\pi}, \tag{43}
$$

$$
I^{+-}_{E1} = \frac{2}{\pi}\int_{-\pi/2}^{\pi/2}\cos^2\phi\sin\phi\sin(2\phi)\,d\phi = \frac{16}{15\pi}, \tag{44}
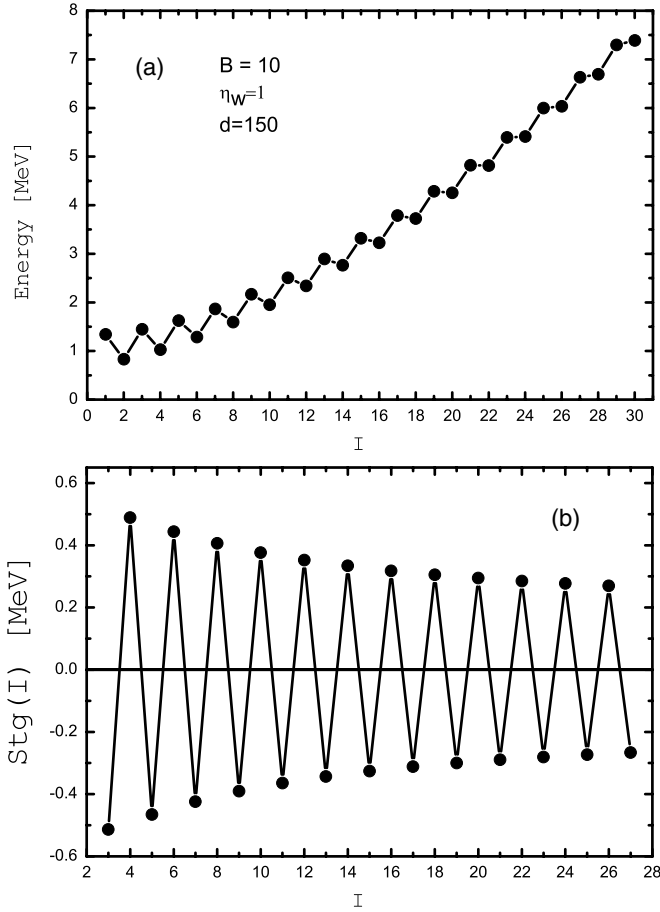$$

FIG. 11. Schematic energy levels (a) and staggering pattern (b) for the spectrum of Eq. (34) with $n = 0$. The parameter values are shown in (a), B is given in $\hbar^2/\text{MeV}$, d is in $\hbar^2$ MeV^{-1}, whereas η_w is dimensionless.

$$I_{E3}^{+-} = \frac{2}{\pi} \int_{-\pi/2}^{\pi/2} \cos\phi \, \sin\phi \, \sin(2\phi) \, d\phi = \frac{1}{2}. \qquad (45)$$

The notations $(++), (--)$, and $(+-)$ correspond to the parities of the functions $\varphi^\pm(\phi)$ included in the integration.

As a result, the reduced $E1$, $E2$, and $E3$ transition probabilities between levels with $|n_i I_i\rangle$ and $|n_f I_f\rangle$ are given by the expressions

$$B(E1, I_i \to I_f) = b_1 \langle I_i 010|I_f 0\rangle^2 S^2(E1, I_i \to I_f), \qquad (46)$$

$$B(EL, I_i \to I_f) = b_L \langle I_i 0L0|I_f 0\rangle^2 S^2(EL, I_i \to I_f), \qquad (47)$$

where

$$S(E1, I_i \to I_f) = \int_0^\infty d\eta \, \psi_{n_f}^{I_f}(\eta) \eta^3 \psi_{n_i}^{I_i}(\eta), \qquad (48)$$

$$S(EL, I_i \to I_f) = \int_0^\infty d\eta \, \psi_{n_f}^{I_f}(\eta) \eta^2 \psi_{n_i}^{I_i}(\eta), \qquad (49)$$

with $L = 2, 3$. In Eq. (47) the values of the integrals (42), (43), and (45) are included in the constant b_L. In Eq. (46) the constant [Eq. (44)] is included in b_1. We remark that if values

of different kinds of transition probabilities are compared, or if branching ratios are considered, Eqs. (42)–(45) should be taken into account explicitly.

In the case of transitions between states of the yrast alternating parity band, $|0I_i\rangle$ and $|0I_f\rangle$ (with $n_i = n_f = 0$), we obtain the integrals in Eqs. (48) and (49) in the following simple analytic form

$$S(E1, I_i \to I_f) = \frac{1}{a^2} \frac{\Gamma(s_i + s_f + 2)}{\sqrt{\Gamma(2s_i + 1)\,\Gamma(2s_f + 1)}}, \qquad (50)$$

$$S(EL, I_i \to I_f) = \frac{1}{a^{3/2}} \frac{\Gamma\left(s_i + s_f + \frac{3}{2}\right)}{\sqrt{\Gamma(2s_i + 1)\,\Gamma(2s_f + 1)}}, \qquad (51)$$

where $s_i = (1/2)\sqrt{k_i^2 + \widetilde{X}(I_i)}$, $s_f = (1/2)\sqrt{k_f^2 + \widetilde{X}(I_f)}$, and $a = \sqrt{BC}/\hbar$.

In the case of the infinite square well potential [case (c)], the model wave function is of the form

$$\Phi_{v,n,IM}^\pm(\eta, \phi) = c_{v,n} J_v(\kappa_{v,n}\eta)\sqrt{\frac{2I + 1}{32\pi^2}} D_{0,M}^I(\theta)\varphi^\pm(\phi), \qquad (52)$$

whereas the integrals over the variable η read

$$S(E1, I_i \to I_f) = \int_0^\infty d\eta \, J_{v_i}(\kappa_{v_i, n_i}\eta)\eta^3 J_{v_f}(\kappa_{v_f, n_f}\eta); \qquad (53)$$

$$S(EL, I_i \to I_f) = \int_0^\infty d\eta \, J_{v_i}(\kappa_{v_i, n_i}\eta)\eta^2 J_{v_f}(\kappa_{v_f, n_f}\eta). \qquad (54)$$

In general, the above formalism can be applied for a detailed analysis of the electric transition rates in spectra where the collective quadrupole-octupole dynamics carries the characteristics outlined in the cases (a)–(c) of our study. In Figs. 12 and 13 we illustrate its application to $E2$ transition probabilities in the nuclei ^{150}Nd, ^{152}Sm, ^{154}Gd, and ^{156}Dy, as well as to the $E1$ transitions in ^{152}Sm, in the framework of case (a). The results are obtained with the parameter sets given in Fig. 7. The quantity $a = \sqrt{BC}/\hbar$, appearing in Eqs. (50) and (51), has been considered as a fitting parameter. The constant b_1 in Eq. (46) has been determined so as to scale the theoretical $E1$ transition values with respect to the experimental data and takes the value $b_1 = 1.2 \times 10^{-6}$, whereas the constants b_L in Eq. (47) have been set equal to 1.

We see a good agreement between theory and experiment for the $B(E2)$ values in ^{150}Nd [Fig. 12(a)], ^{152}Sm [Fig. 13(a)], and ^{154}Gd [Fig. 12(b)]. In Fig. 12(c), the theoretical $E2$ transition probabilities in ^{156}Dy are compared to two different sets of experimental data, Refs. [29] and [30] (with no error bars reported in Ref. [30]. We see that the theoretical values follow only the overall increase of the experimental data. We should, however, remark that the two sets of data diverge essentially, especially at the higher angular momenta. There is also some discrepancy between theory and experiment in the $E1$ transition values in ^{152}Sm [Fig. 13(b)]. The results in Figs. 12(c) and 13(b) suggest that further examination of the formalism, as well as of the experimental data, may be necessary. The further analysis of data on electric transitions in a wider range of nuclei will be the subject of future work.
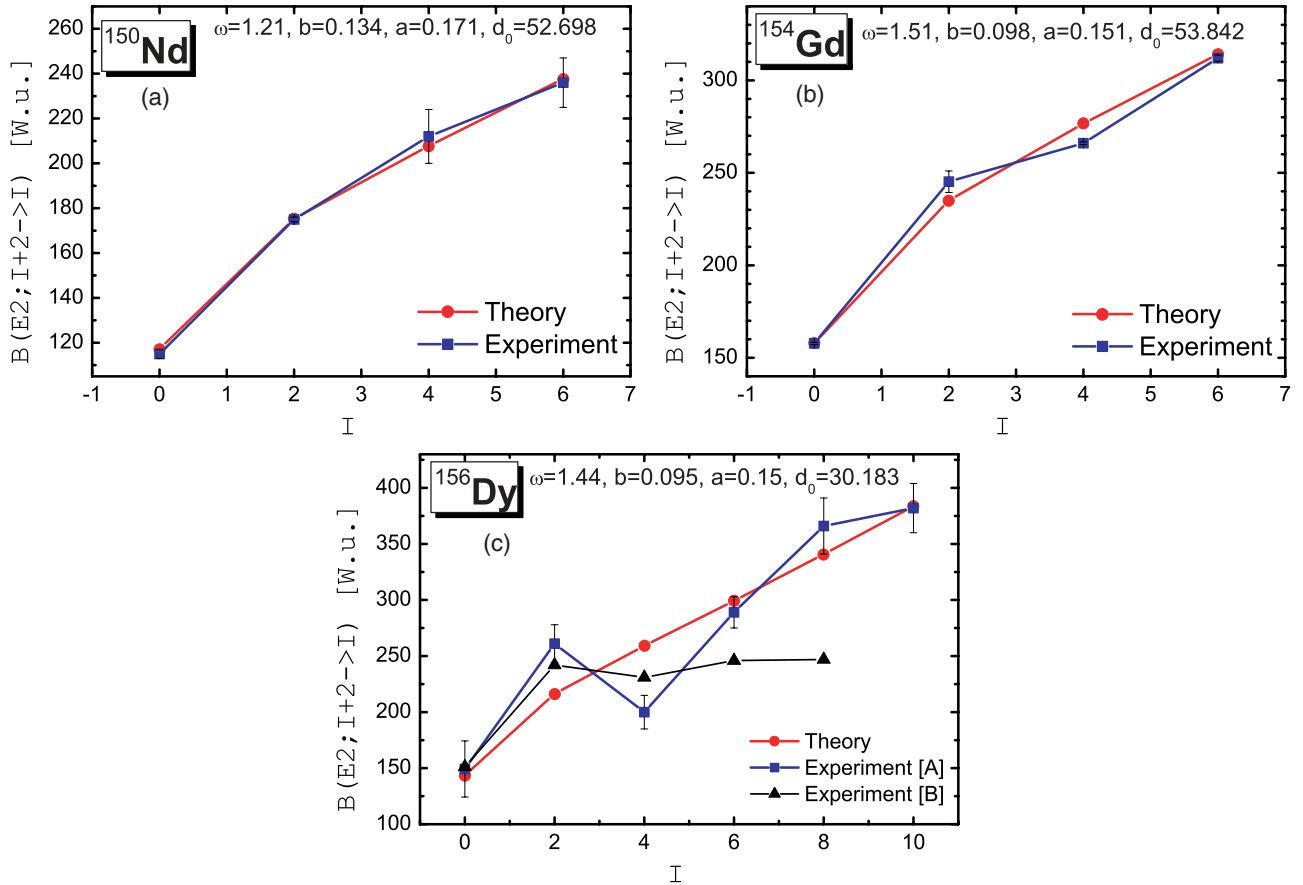
FIG. 12. (Color online) Theoretical and experimental $B(E2)$ transition probabilities (in W.u.) as functions of the angular momentum in the alternating parity spectra of ^{150}Nd, ^{154}Gd, and ^{156}Dy. The data for ^{150}Nd, ^{154}Gd, and for Experiment A in ^{156}Dy are from Ref. [29]; Experiment B in ^{156}Dy is from Ref. [30]. The theoretical results are obtained by Eq. (47). See Sec. V for further discussion.

VI. INFLUENCE OF THE γ DEFORMATION MODE ON THE β_2-β_3 COLLECTIVE MOTION

As it has been mentioned in Sec. IV, the present model framework does not include the γ degree of freedom. Here we briefly discuss the possible ways in which this can be done and shortly estimate the influence of the γ deformation mode on the collective motion in the β_2-β_3 space. The rotation energy of a system with presence of axial and triaxial quadrupole modes (β_2 and γ) and axial octupole degree of freedom (β_3) can be
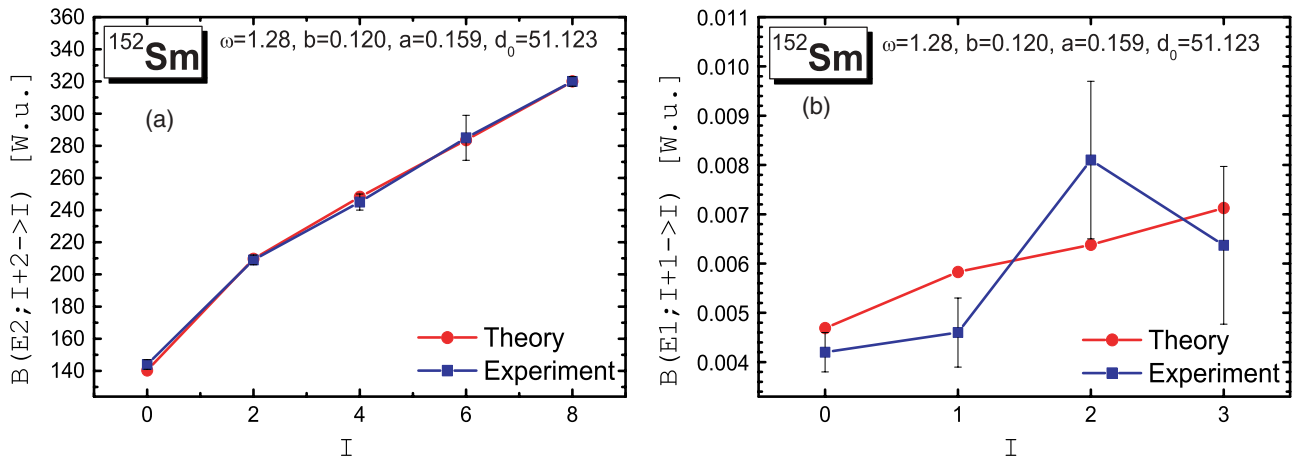

FIG. 13. (Color online) Theoretical and experimental $B(E2)$ (a) and $B(E1)$ (b) transition probabilities (in W.u.) as functions of the angular momentum in the alternating parity spectrum of ^{152}Sm (data from Ref. [29]. The theoretical results are obtained by Eqs. (46) and (47).

given by [13,31]

$$\hat{T}_{\text{rot}} = \frac{1}{2} \sum_{i=1}^{3} \frac{\hat{I}_i^2}{J_i^{(2)} + J_i^{(3)}}, \quad (55)$$

where

$$J_i^{(2)} = 4B_2 \beta_2^2 \sin^2\left(\gamma - \frac{2\pi i}{3}\right), \quad (i = 1, 2, 3) \quad (56)$$

are the moment-of-inertia components of the quadrupole shape about the axes 1, 2, and 3, whereas those of the axially symmetric octupole shape are

$$J_1^{(3)} = J_2^{(3)} = 6B_3 \beta_3^2, \qquad J_3^{(3)} = 0. \quad (57)$$

A simple estimation of the γ influence can be done by assuming small variations of the system around $\gamma = 0$, as in the case of the X(5) model [12]. Then the quadrupole moment-of-inertia components (56) can be taken as

$$J_1^{(2)} = J_2^{(2)} = 3B_2 \beta_2^2, \qquad J_3^{(2)} = 4B_2 \beta_2^2 \sin^2 \gamma. \quad (58)$$

As a result the rotation energy (55) obtains the form

$$\hat{T}_{\text{rot}} = \frac{1}{2}\left(\frac{\hat{I}^2 - \hat{I}_3^2}{3B_2 \beta_2^2 + 6B_3 \beta_3^2} + \frac{\hat{I}_3^2}{4B_2 \beta_2^2 \sin^2 \gamma} \right). \quad (59)$$

The first term in Eq. (59) corresponds to the centrifugal term in the quadrupole-octupole potential described in Eq. (2). The second term in Eq. (59) provides the influence of the γ mode on the potential. After taking into account Eq. (59) with $d_2 = 3B_2$ and $d_3 = 6B_3$, and by including a γ-oscillation term, Eq. (2) can be generalized in the form

$$U(\beta_2, \beta_3, \gamma, I) = \frac{1}{2}C_2\beta_2{}^2 + \frac{1}{2}C_3\beta_3{}^2 + \frac{1}{2}C_2'\gamma^2$$
$$+ \frac{X(I) - K^2/2}{d_2\beta_2^2 + d_3\beta_3^2} + \frac{3K^2/2}{4d_2\beta_2^2 \sin^2 \gamma}, \quad (60)$$

where K is the projection of the angular momentum on the body-fixed z-axis. Then for a fixed value of γ the extremum conditions (3) and (4) in Sec. II provide the following cases for the bottom of the potential (60) in the β_2-β_3 space.

(a) $\beta_{3\text{min}} = 0$ with

$$\beta_{2\text{min}} = \pm\left\{ \frac{2}{d_2 C_2}\left[X(I) + \frac{K^2}{2}\left(\frac{3}{4\sin^2 \gamma} - 1 \right) \right] \right\}^{1/4}. \quad (61)$$

(b) $\beta_{2\text{min}} \neq 0$ and $\beta_{3\text{min}} \neq 0$ with the condition

$$C_2 = \frac{[2X(I) - K^2]d_2}{\left(d_2\beta_{2\text{min}}^2 + d_3\beta_{3\text{min}}^2\right)^2} + \frac{3K^2}{4d_2\beta_{2\text{min}}^4 \sin^2 \gamma}$$

and

$$C_3 = \frac{[2X(I) - K^2]d_3}{\left(d_2\beta_{2\text{min}}^2 + d_3\beta_{3\text{min}}^2\right)^2}. \quad (62)$$

The following comments can be done on the above result:

(i) The appearance of β_2^2 in the denominator of the second term in Eq. (60) divides the β_2-β_3 space into two half-spaces, $\beta_2 > 0$ and $\beta_2 < 0$, separated by an infinite

potential barrier at $\beta_2 = 0$. For this reason the potential minimum with $\beta_{2\text{min}} = 0$ and $\beta_{3\text{min}} \neq 0$ does not appear.

(ii) Equations (61) and (62) illustrate the ways in which the term involving the γ deformation mode can shift the position of the potential minima in the β_2-β_3 space [compare with cases (i)–(iii), including Eq. (6) in Sec. II]. Note that for $K = 0$ the influence of the γ mode on the β_2-β_3 potential shape automatically disappears. This is a limit in which the β_2 and γ degrees of freedom are weakly coupled and can be adiabatically separated, *which is implied in the framework of the present work.* The involvement of the $K = 2$ configurations in the collective motion implies the consideration of a strong β_2-γ coupling [32].

(i) The involvement of the γ degree of freedom in the above way would influence the correlation between the axial β_2 and β_3 variables because of the appearance of the second term in C_2 [Eq. (62)], as a consequence of the last term in Eq. (60). Now, in terms of the polar variables, the potential will depend on both η and ϕ, so that the variables in the Schrödinger equation cannot be directly separated. This could be done in a way similar to the adiabatic separation of the β and γ degrees of freedom in the X(5) model framework [12], as well as in the framework of the AQOA model [33]. Alternatively, the problem could be solved numerically in a way similar to the approach of Ref. [32].

A more general way to examine the influence of the γ deformation mode on the quadrupole-octupole motion of the system could be based on the complete form [Eq. (56)] of the quadrupole moment-of-inertia components, so that the γ variable would not be limited in the vicinity of zero. Furthermore, nonaxiality of the octupole degree of freedom can be considered. Any efforts in these directions should be based on numerical solution of the problem.

VII. SUMMARY AND CONCLUSIONS

The present study outlines some dynamical properties of a system with *simultaneously* manifesting quadrupole and octupole degrees of freedom. We remark that the obtained results represent a restricted class of *exact analytic* solutions of the problem. This is because of the correlation (16) between the mass and the inertial parameters, which essentially simplifies the Hamiltonian in Eq. (11) in the form of Eq. (17). In addition, the correlation [Eq. (6)] between the inertial and oscillator parameters brings the potential in a form depending on the "effective deformation" variable η only, and not on the relative "angular" variable ϕ, thus allowing an *exact* separation of variables in the Schrödinger equation. As it is explained in Sec. IV, the above correlations provide a *coherent interplay* between the quadrupole and octupole collective modes. In this respect, the presently considered potentials suggest some specific properties of quadrupole-octupole collectivity, which can be developed in various nuclear regions.

However, despite the above limitations (the necessary price we pay for solving the problem exactly) we were able to identify a region of nuclei where the assumed "equal" presence of quadrupole and octupole degrees of freedom can take place in the collective motion. We found that the structure of the

spectrum in the case of the potential (12), illustrated in Fig. 6, is similar to the structure of alternating parity bands in some rare-earth nuclei. On this basis, we have reproduced quite accurately the energy levels and the staggering patterns in the nuclei ^{150}Nd, ^{152}Sm, ^{154}Gd, and ^{156}Dy, as demonstrated in Figs. 7 and 8. In these spectra the reduction of the staggering amplitude indicates the *trend of forming octupole deformations* toward the higher angular momenta. However, the slow decrease of the parity effect does not allow this to happen at reasonable (observed) angular momenta. The $B(E2)$ transition probabilities have been also described with a reasonable accuracy (Figs. 12 and 13, whereas the result for $B(E1)$ transition probabilities in ^{152}Sm [Fig. 13(b)] suggests further tests of the formalism and analysis of additional experimental data.

We remark that the energy expression (23) cannot reproduce the complicated beat staggering effects observed in the octupole bands of light actinide nuclei [34]. The latter have been described [14], with good accuracy, by the use of the quadrupole-octupole rotation model [35]. Thus, compared to the light actinide region, the application of expression (23) indicates a different behavior of the quadrupole-octupole collectivity in the rare-earth nuclei, with a *less developed octupole deformation* and a *more strongly pronounced octupole vibration mode*. The present analysis suggests that in this case the *coherent (equal) contribution* of quadrupole and octupole oscillations can take place in the collective motion of nuclei.

The potentials with fixed energy minima [cases (b) and (c)] can be related generally to a situation in which the vibrational and rotational degrees of freedom are weakly coupled. Then the rotational angular momentum slightly affects the quadrupole-octupole vibration motion, which suggests a constant (or nearly constant) behavior of the staggering amplitude. In particular this is well seen in the case (b2) where the direct contribution of the rotational motion is excluded. Thus, the spectrum illustrated in Fig. 10 suggests an essentially quadrupole-octupole *vibrational* motion of the system. Cases (b1) and (c), in which the rotational mode is taken into account, suggest quadrupole-octupole vibrations with an adiabatically manifested *rotational* motion. We remark that the constant staggering patterns, illustrated in Figs. 9 and 10, are in some meaning idealistic cases, as far as the current experimental data do not show such a strong persistence of the parity effect at high angular momenta. However, the square-well potential of case (c) appears to be applicable to examining the possible critical behavior of the quadrupole-octupole collectivity in different nuclear regions. Studies in this direction have been implemented recently in the light actinide nuclei [33]. We suggest that further analysis of experimental data for quadrupole-octupole spectra would be of use for testing the prediction of the staggering pattern illustrated in Fig. 11 for the case of the square-well potential (15).

It is important to note that the present exactly solvable model can be naturally extended, beyond the "coherent interplay" assumption, to a more general nonanalytic problem in the following two ways. First, we can release the correlation [Eq. (6)] between the inertial and oscillator parameters, allowing the potential to depend on the variable ϕ. Then the problem can still be transformed into a form having an analytical solution, by performing an "approximate" separation of variables, as done in Ref. [33] and in the framework of the X(5) symmetry model [12]. The second extension would be to release the correlation (16) between the mass and inertial parameters. This would allow us to examine different ways in which the coupled quadrupole and octupole degrees of freedom enter the collective motion. In this case, however, more sophisticated mathematical and numerical techniques have to be sought to solve the problem.

Finally, we also remark that the developed formalism contains several limits. Thus, when the quadrupole variable is frozen to some stable quadrupole deformation, the potentials and the spectra of the cases (a)–(c) transform to the respective ones appearing in the one-dimensional problem [14,15]. Another interesting limit can be obtained by appropriate parameter values, for which the difference Δk^2 is negligible compared to $\widetilde{X}(I)$ for all angular momentum values. Then the staggering effect vanishes, and the odd and even angular momentum sequences appear in a single nonperturbed collective band. For example, if such a transition is performed in case (c), the spectrum presented in Fig. 11 is reduced to the structure supposed to correspond to the transition between octupole vibrations and stable octupole deformation, in which a single octupole band is formed [33]. It is also of interest to take into account the nonaxiality of the quadrupole and/or the octupole degree of freedom, to examine how the present results are modified. Studies in these directions are the subject of further work.

[1] A. Bohr and B. R. Mottelson, *Nuclear Structure* (Benjamin, New York, 1975), Vol. II.

[2] I. Ahmad and P. A. Butler, Annu. Rev. Nucl. Part. Sci. **43**, 71 (1993).

[3] P. A. Butler and W. Nazarewicz, Rev. Mod. Phys. **68**, 349 (1996).

[4] H. J. Krappe and U. Wille, Nucl. Phys. **A124**, 641 (1969).

[5] G. A. Leander, R. K. Sheline, P. Möller, P. Olanders, I. Ragnarsson, and A. J. Sierk, Nucl. Phys. **A388**, 452 (1982).

[6] R. Jolos, P. von Brentano, and F. Dönau, J. Phys. G **19**, L151 (1993).

[7] R. V. Jolos and P. von Brentano, Phys. Rev. C **49**, R2301 (1994).

[8] A. Ya. Dzyublik and V. Yu. Denisov, Yad. Fiz. **56**, 30 (1993) [Phys. At. Nucl. **56**, 303 (1993)].

[9] V. Yu. Denisov and A. Ya. Dzyublik, Nucl. Phys. **A589**, 17 (1995).

[10] R. F. Casten and N. V. Zamfir, Phys. Rev. Lett. **87**, 052503 (2001).

[11] R. M. Clark, M. Cromaz, M. A. Deleplanque, M. Descovich, R. M. Diamond, P. Fallon, R. B. Firestone, I. Y. Lee, A. O. Macchiavelli, H. Mahmud, E. Rodriguez-Vieitez, F. S. Stephens, and D. Ward, Phys. Rev. C **68**, 037301 (2003).

[12] F. Iachello, Phys. Rev. Lett. **87**, 052502 (2001).

[13] J. P. Davidson, *Collective Models of the Nucleus* (Academic Press, New York, 1968).

[14] N. Minkov, P. Yotov, S. Drenska, and W. Scheid, J. Phys. G: Nucl. Part. Phys. **32**, 497 (2006).

[15] P. G. Bizzeti and A. M. Bizzeti-Sona, Phys. Rev. C **70**, 064319 (2004).

[16] P. M. Davidson, Proc. R. Soc. London Ser. A **135**, 459 (1932).

[17] J. P. Elliott, J. A. Evans, and P. Park, Phys. Lett. **B169**, 309 (1986).

[18] D. J. Rowe and C. Bahri, J. Phys. A **31**, 4947 (1998).

[19] E. der Mateosian and J. K. Tuli, Nucl. Data Sheets **75**, 827 (1995).

[20] A. Artna-Cohen, Nucl. Data Sheets **79**, 1 (1996).

[21] C. W. Reich and R. G. Helmer, Nucl. Data Sheets **85**, 171 (1998).

[22] C. W. Reich, Nucl. Data Sheets **99**, 753 (2003).

[23] J. M. Eisenberg and W. Greiner, *Nuclear Theory: Nuclear Models* (North-Holland, Amsterdam, 1970), Vol. I.

[24] C. Dorso, W. Myers, and W. Swiatecki, Nucl. Phys. **A451**, 189 (1986).

[25] W. Myers and W. Swiatecki, Nucl. Phys. **A531**, 93 (1991).

[26] V. Yu. Denisov, Yad. Fiz. **49**, 644 (1989) [Sov. J. Nucl. Phys. **49**, 399 (1989)].

[27] V. Yu. Denisov, Yad. Fiz. **55**, 2647 (1992) [Sov. J. Nucl. Phys. **55**, 1478 (1992)].

[28] A. R. Edmonds, *Angular Momentum in Quantum Mechanics* (Princeton University Press, Princeton, 1957).

[29] http://www.nndc.bnl.gov/ensdf/

[30] A. Dewald, O. Möller, D. Tonev, A. Fitzler, B. Saha, K. Jessen, S. Heinze, A. Linnemann, J. Jolie, K. O. Zell, P. von Brentano, P. Petkov, R. F. Casten, M. Caprio, J. R. Cooper, R. Krücken, V. Zamfir, D. Bazzacco, S. Lunardi, C. Rossi Alvarez, F. Brandolini, C. Ur, G. de Angelis, D. R. Napoli, E. Farnea, N. Marginean, T. Martinez, and M. Axiotis, Eur. Phys. J. A **20**, 173 (2004).

[31] V. M. Maslov, Yu. V. Porodzinskij, N. A. Tetereva, M. Baba, and A. Hasegawa, Nucl. Phys. **A764**, 212 (2006).

[32] M. A. Caprio, Phys. Rev. C **72**, 054323 (2005).

[33] D. Bonatsos, D. Lenis, N. Minkov, D. Petrellis, and P. Yotov, Phys. Rev. C **71**, 064309 (2005).

[34] D. Bonatsos, C. Daskaloyannis, S. B. Drenska, N. Karoussos, N. Minkov, P. P. Raychev, and R. P. Roussev, Phys. Rev. C **62**, 024301 (2000).

[35] N. Minkov, S. B. Drenska, P. P. Raychev, R. P. Roussev, and D. Bonatsos, Phys. Rev. C **63**, 044305 (2001).